

Photoemission and photoabsorption study of C₆₀ adsorption on Cu(111) surfaces

Ku-Ding Tsuei

*Synchrotron Radiation Research Center, Hsinchu, Taiwan 300, Republic of China
and Department of Physics, National Tsing-Hua University, Hsinchu, Taiwan 300, Republic of China*

Jih-Young Yuh

*Synchrotron Radiation Research Center, Hsinchu, Taiwan 300, Republic of China
and Department of Electrical Engineering, National Tsing-Hua University, Hsinchu, Taiwan 300, Republic of China*

Chyuan-Tsyrr Tzeng

Department of Electrical-Optical Engineering, National Chiao-Tung University, Hsinchu, Taiwan 300, Republic of China

Ren-Yu Chu

Department of Physics, National Tsing-Hua University, Hsinchu, Taiwan 300, Republic of China

Shih-Chun Chung and King-Lung Tsang

Synchrotron Radiation Research Center, Hsinchu, Taiwan 300, Republic of China

(Received 11 August 1997)

We have carried out an extensive study of C₆₀ adsorption on Cu(111) surfaces using low-energy electron diffraction, photoemission, and x-ray-absorption spectroscopy. It is found that in valence-band photoemission a state forms right below the Fermi energy for an annealed, well-ordered monolayer, similar to the case of K-doped C₆₀. This peak disperses across the Fermi energy at off normal emission geometry. The spectra of carbon core-level photoemission show that the line shape is highly asymmetric with a metalliclike tail. The carbon near-edge absorption spectra show that the lowest unoccupied molecular orbital (LUMO) is attenuated, and a clear Fermi edge jump appears at the absorption onset. This evidence indicates that charge transfers from the substrate to the C₆₀ molecular orbitals and the overlayer becomes metallic. The amount of charge transfer can be determined to be 1.5–2 electrons per molecule from both the area of the occupied LUMO in photoemission and the peak shift in near-edge absorption spectra. It has been reported that many metal surfaces with originally different work functions covered by a monolayer of C₆₀ have a similar work function of about 5 eV. We suggest that the measured work functions are due to the metallic C₆₀ overlayers and are similar regardless of the metal substrates. This is in line with the reported alignment of monolayer energy levels to substrate Fermi energy. Since the work functions are similar, the energy levels with respect to the vacuum level are also similar. Finally we compare near-edge x-ray-absorption with inverse photoemission spectroscopy to address the screening effects. [S0163-1829(97)05348-4]

I. INTRODUCTION

One of the most fascinating observations in the studies of C₆₀ is the high temperature superconductivity in the alkali-doped solids.^{1,2} The electronic structure of these compounds has been measured by photoemission, inverse photoemission, and x-ray-absorption spectroscopies.^{3,4} These studies indicate that with continuous K doping the lowest unoccupied molecular orbital (LUMO) of C₆₀ becomes gradually filled. This observation lends strongest support to the idea of charge transfer from the K 4s electrons to the LUMO. For example, the K-doped compounds are labeled K_xC₆₀. For $x=6$ the LUMO band is fully occupied producing an insulating state. For $x=3$ the LUMO band is half-filled, and the compound is believed to be a normal conductor at room temperature and converts to superconducting phase at 19 K.^{1,2} The latter compound has also been proposed to be a Mott-Hubbard insulator.⁵ In addition, the compound K₄C₆₀ was found to be an insulator, in contradiction to band theory.⁶

There is increasing interest in the study of the C₆₀ metal interface. All results concluded that the interaction is strong chemisorption rather than van der Waals as in C₆₀ solids. A photoemission spectroscopy (PES) study of C₆₀ on metal films found that the C₆₀ molecular orbitals are aligned with the substrate Fermi levels rather than the vacuum levels, despite large variations in the work function.⁷ This was interpreted as a partial filling of the LUMO due to charge transfer, as shown by broadening and rigid shift toward the Fermi level of the unoccupied MO's in the system of C₆₀ on a Au film observed in inverse photoemission spectroscopy (IPES). There are a few cases of identifying charge transfer by observing directly a state right below the Fermi level in PES. Another PE study of C₆₀ on noble-metal films revealed peaks in Ag and Cu but not in Au films, in contrast to the IPES result.⁸ The combined Raman-scattering study showed the largest energy shift in Ag, and the smallest in Au. Peaking below the Fermi level was also seen in C₆₀ on Ag(111).⁹ However, no peaks were observed in PES in Au(110) (Ref. 10) and Al(111).¹¹ Both studies combined with near-edge

x-ray-absorption spectroscopy (NEXAFS) and core-level PES. The former emphasized the hybridization between the LUMO and substrate states, while the latter concluded that the bonding nature is covalent. A recent IPES study on Cu(111) concluded on the charge transfer and metallicity of the first layer.¹² A shift of carbon core-level binding energy and of NEXAFS peaks to lower values was also claimed to be due to charge transfer.^{7,13,14} The amount of charge transfer has been measured in several C₆₀ on metal systems, using vibrational energy shifts, in electron-energy-loss spectroscopy (EELS). It was concluded that the transferred amount is 2 ± 1 electrons per molecule in Ni(110),¹⁵ 1 ± 1 electrons in Au(110),^{15,16} and less than 0.8 electrons in Pt(111).¹⁷ Charge transfer or at least strong chemical bonding was also found in several other studies.^{18–25} In the system of C₆₀ on Rh(111), a work-function lowering was observed, and it was suspected that the net charge transfer is from the highest occupied molecular orbitals (HOMO's) to the substrate,²⁶ in contrast to all other systems. A number of scanning tunneling microscopy (STM) studies were performed.^{27–32} In particular, the study of C₆₀ on Cu(111) suggested that the monolayer of C₆₀ is metallic instead of semiconducting.²⁷

We choose Cu(111) as the substrate to study the interaction between C₆₀ and a metal surface. The reasons are twofold. First, there is a bulk projected band gap around the Fermi energy at the $\bar{\Gamma}$ point in Cu(111). As a result, the background emission from the substrate should be very low, and any peak due to charge transfer to C₆₀ must be easily observed in angle-resolved photoemission. This is likely why the charge-transfer peak could not be detected in many previous studies. Furthermore, C₆₀ forms a commensurate structure on Cu(111) surfaces. This eliminates complications due to multiple-site adsorption.

We focus in this paper on the electronic structure of a monolayer of C₆₀ chemisorbed on a Cu(111) surface. The techniques used were valence-band and core-level PES, NEXAFS, and low-energy electron diffraction (LEED). We found in these studies that a charge-transfer model is consistent with all the spectroscopic results. In Sec. II we outline the experimental procedures. In Sec. III, the results are discussed in the order of valence-band PES, carbon 1s core-level PES, and NEXAFS; the work function of the monolayer films and the comparison of NEXAFS with IPES are presented separately. Finally we summarize our conclusions in Sec. IV.

II. EXPERIMENT

The experiment was carried out at the Synchrotron Radiation Research Center in Hsinchu, Taiwan using low-energy spherical grating monochromator (LSGM) and high-energy spherical grating monochromator (HSGM) beamlines. The angle-resolved valence photoemission was carried out in a UHV chamber equipped with LEED and a 36-mm-radius hemispherical analyzer mounted on a two-axis goniometer. The angular acceptance is $\pm 1^\circ$.³³ Photon energies from 16 to 25 eV were used. The overall resolution was 0.12 eV, judging from the width of the Cu(111) surface state. The core-level photoemission and absorption measurements were carried out in a separate chamber with a Vacuum Science Workshop (VSW) EA-125 hemispherical analyzer mounted

perpendicular to the incident light. For carbon core-level photoemission, a photon energy of 330 eV was used to maximize the intensity. The overall resolution was better than 0.4 eV, which was the width of C 1s emission from a thick film. For the absorption measurement the carbon Auger signal was monitored from the same analyzer, and normalized to a clean surface total yield spectrum. The photon energy was calibrated by photoemission from the second-order light. It was also checked by monitoring the mesh current in front of the sample, and comparing the characteristic absorption dips due to carbon contamination of the beamline. The crystal was cleaned by 1-keV Ar-ion sputtering, and annealing was monitored by a thermal couple clamped to the sample surface. The C₆₀ used was high-purity (>99.5%), commercially available powder. It was evaporated from a homemade resistivity heated Ta evaporator controlled by a thermal couple and a quartz-crystal monitor. It was thoroughly degassed before deposition, and the pressure rise was less than 2×10^{-10} Torr. The evaporation rate was kept lower than 5 min per layer. A higher rate caused significant non-layer-by-layer growth even at a submonolayer coverage. The evaporation and measurements were done at room temperature (RT). As in previous studies of STM (Ref. 27) and LEED,¹² deposition at RT causes small domains of 4×4 islands in submonolayer coverage. It has been determined that only threefold hollow sites are occupied.²⁷ The coverage was calibrated by observing the attenuation of a clean Cu(111) surface state or the appearance of a second-layer peak in C 1s photoemission. Annealing to 300 °C can desorb multilayers, leaving only a ML on the surface resulting in a sharp 4×4 LEED pattern.^{12,13} This means much larger well-ordered domains. The C₆₀-C₆₀ distance of the 4×4 structure is 10.21 Å, that is, 1.7% larger than the nearest-neighbor distance of 10.04 Å in the bulk. The work function was obtained by subtracting photoemission spectral width from the known photon energy (He I).

III. RESULTS AND DISCUSSION

A. Valence-band photoemission and Fermi-level crossing

Figure 1 shows the valence-band normal-emission spectra as a function of C₆₀ coverage deposited at RT using 21-eV photons. The bottom curve is from a clean surface. The strong two-peak group between 2- and 4-eV binding energies is due to Cu *d* band. The small peak at 0.4-eV binding energy is the surface state located in the bulk-projected band gap from about 0.9-eV binding energy and above. Upon C₆₀ deposition, peaks due to its molecular orbitals grow in intensity, and the substrate features diminish. The peak at 1.7-eV binding energy is from the HOMO. It shifts toward higher binding energy as the second layer starts growing, in agreement with previous measurements. Finer scans close to the Fermi energy region show a linear decrease of the Cu(111) surface-state intensity, and a linear increase of the intensity at the Fermi level. This behavior is consistent with island growth of C₆₀ at RT; the surface-state intensity comes from the substrate region uncovered by C₆₀, while the Fermi-level emission is mainly from C₆₀ islands. The intensity at the Fermi energy decreases beyond 1 ML. This is because the insulating multilayer C₆₀ makes no contribution to the emis-

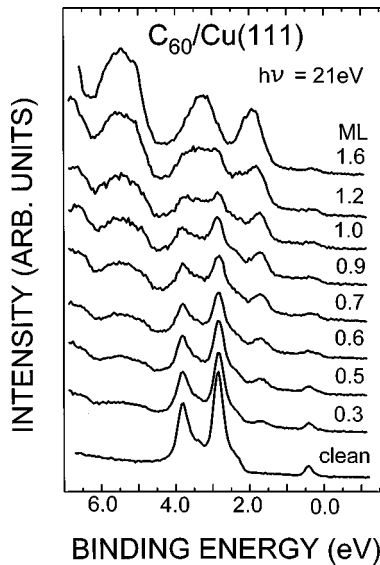


FIG. 1. Coverage dependence of normal-emission photoelectron spectra of C_{60} on Cu(111) deposited at room temperature. The photon energy was 21 eV, and the incident angle was 45° . These spectra are normalized to the intensity above the Fermi energy.

sion, while it attenuates the emission intensity from the interface above the energy of the HOMO. This is consistent with the IPES study.¹²

Annealing causes a dramatic change in the low-binding-energy region, and the effect is shown in the spectra in Fig. 2. The bottom curve displays a normal-emission spectrum from a clean Cu(111) surface at 21-eV photon energy. Except at the surface state there is almost no emission in the band gap. The middle curve corresponds to a near-1-ML film, as deposited. The surface state is almost completely attenuated. The Fermi edge jump can clearly be seen. The tail below 1.2-eV binding energy is part of the HOMO. There are no other discernible peaks that can be identified. The top curve taken at 20-eV photon energy is obtained by

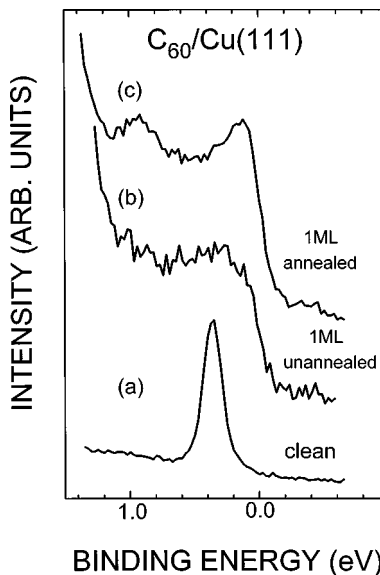


FIG. 2. Comparison of normal-emission spectra near the Fermi level for (a) a clean surface, $h\nu=21$ eV; (b) an unannealed 1-ML film, $h\nu=21$ eV; and (c) an annealed 1-ML film, $h\nu=20$ eV.

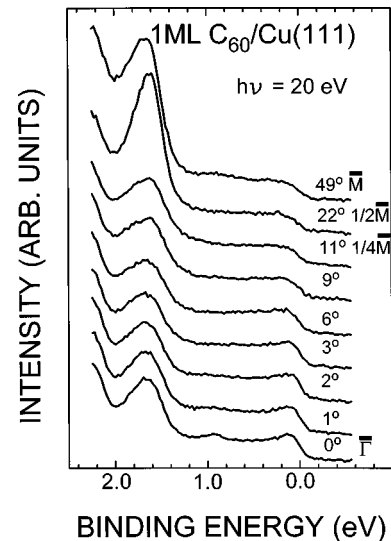


FIG. 3. Angular dependence of photoemission spectra from 1-ML C_{60} on Cu(111). The emission angles are noted on the right. The \bar{M} point refers to the zone boundary of the clean surface. For the 4×4 overlayer $\frac{1}{4}\bar{M}$ becomes the zone boundary, and $\frac{1}{2}\bar{M}$ and \bar{M} are equivalent to $\bar{\Gamma}$.

annealing a 2-ML film to 300°C to desorb the second layer. For this ML film the Fermi level cutoff becomes more prominent, and a sharp peak at 0.15 eV appears right below the Fermi energy. In addition, there appears another peak at 0.9 eV. It is found that this latter peak resonates in a narrow photon energy range between 18 and 22 eV, and disappears in a flat background outside this range. Submonolayer C_{60} films were prepared, and subsequent annealing showed the coexistence of a clean surface state, the 0.15-eV peak, and this 0.9-eV peak, indicating that the appearance of this peak is associated with the ordering of the 4×4 islands.

The dispersion spectra of these two peaks along with the HOMO measured at 20-eV photon energy are plotted in Fig. 3. The symmetry point \bar{M} refers to the substrate, and the fractions are measured in \mathbf{k} space along the $\bar{\Gamma}-\bar{M}$ direction. As the overlayer unit cell vectors are four times larger than that of the substrate $\frac{1}{4}\bar{M}$ is actually the zone boundary, and $\frac{1}{2}\bar{M}$ and \bar{M} become the center of higher Brillouin zones associated with the overlayer. It is seen that the 0.15-eV peak attenuates away from normal emission. The 0.9-eV peak disappears more quickly at off-normal geometry, and reappears at \bar{M} but not at $\frac{1}{2}\bar{M}$. We find that this is due to the matrix element effect. When a 22-eV photon was used, it appeared in all these symmetry-equivalent $\bar{\Gamma}$ points.

The peak right below the Fermi energy at 0.15 eV is of primary interest. Its intensity diminishes quickly away from normal emission, presumably dispersing across the Fermi level. The difficulty of measuring a finite dispersion could be twofold. One problem is the lack of resolution in the measurement. The other is that there are three LUMO's transforming like three p orbitals in group theory. Adsorption removes the degeneracy and the charge transfer to one LUMO could be different from the other two. In an IPES study of the same system, no apparent Fermi-level crossing was observed,¹² and this is likely due to the relatively poorer energy and angular resolution associated with this technique.

Because this 0.15-eV peak appears, after annealing, to achieve a highly ordered overlayer, one may interpret it as due to substrate emission folded back by the overlayer lattice, as observed in the Li/Be system.³⁴ A detailed study shows that no peak right below the Fermi level, either from a clean or annealed C_{60} -covered surface at \bar{M} and $\frac{1}{2}\bar{M}$, can account for the peak at normal emission. Thus it must be associated with the overlayer electronic structure. The finite Fermi-level jump and peak crossing assure us that the C_{60} overlayer becomes metallic. In the case of alkali-doped C_{60} , it is observed that the LUMO in IPES disappears across the Fermi level, and a peak appears at the Fermi level in PES. Charge transfer from alkali atoms to the C_{60} LUMO is the widely accepted explanation. In our case a similar peak can be observed, but not as prominently. If the low emission background of a clean surface is subtracted from the normal-emission spectrum of a monolayer surface, and the resulting spectrum is fitted with three components—the HOMO, 0.9 eV, and 0.15 eV peaks, the latter area is about 20% of the HOMO, and corresponds to approximately two electrons. This ratio can only be taken as an approximate value, because we find that it depends upon the photon energy used. This behavior of the photon-energy-dependent cross section has been observed in PES of thick films.³⁵ We thus conclude that charge transfer is a good explanation. We note here that IPES and STM reach a similar conclusion.^{12,27} Changing the incident angle shows that this peak favors p polarization. This implies that the transferred charge is not symmetrically distributed around the center of the molecule.⁷ We emphasize here that the occupied parts of the LUMO of a particular molecule due to charge-transfer overlap with the same parts of neighboring molecules, forming bands; these bands disperse across the Fermi level, causing the two-dimensional monolayer film to become metallic. The intermolecular interaction is no longer van der Waals.

The HOMO appears at 1.7-eV binding energy at normal emission, with a width narrower than that of a 2-ML film. One observes that the HOMO peak shape changes slightly, and the apparent peak position change is less than 0.1 eV in the dispersion spectra. A study of a thick $C_{60}(111)$ film measured 400-meV dispersion using 8-eV photons.³⁶ We note here that our monolayer film is two dimensional instead of three dimensional for the thick film, and the nearest-neighbor distance 10.21 Å of the former is larger than that of the latter. Therefore a smaller dispersion is not surprising. Furthermore we measure higher-kinetic-energy electrons with $\pm 1^\circ$ moderate angular resolution that accounts for about 18% of the distance from zone center to boundary, and tends to smear out some of the dispersion. The shape change in our data reflects partly the dispersion and partly the matrix element effect of the five individual orbitals composed of HOMO's. At any emission angle the width of the HOMO for 1 ML is narrower than that of a thick film. This reflects the lack of dispersion along the z direction, and, more importantly, no interaction between the HOMO and the substrate, unlike Al(111) and Rh(111) systems.^{11,26}

It is more difficult to understand the origin of the 0.9-eV peak. It shows up only between 18- and 22-eV photon energies for an annealed film, disappears even more quickly than the 0.15-eV peak away from normal emission; and reappears at symmetry equivalent $\bar{\Gamma}$ points. We attempt to interpret it

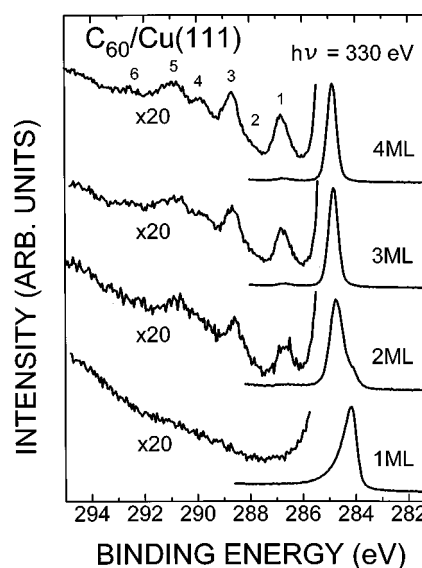


FIG. 4. Carbon $1s$ core-level photoemission spectra at various thicknesses. These spectra are normalized to have the same height as the main peak. On the left are the enlarged spectra of the satellite region. The multiplication factors are shown. The satellites are labeled for discussion in the text.

as originally from the clean substrate surface state modified by the presence of well-ordered C_{60} overlayer. It disperses into the Cu bulk continuum at off-normal emission, so as to disappear quickly. We note here that in an IPES study¹² an image state also only shows up in an annealed, ordered film, not in an unannealed, disordered film.

B. Core-level photoemission and a metallic tail

The carbon $1s$ core-level photoemission spectra of different C_{60} thicknesses are shown in Fig. 4. From a previous study,³⁷ the attenuation length is measured as approximately one layer; thus the intensity is mainly from the top layer. The spectrum of a 4-ML film is identical to the published thick-film results. The main peak has 284.85-eV binding energy with respect to the substrate Fermi level, and a 0.43-eV full-width at half maximum (FWHM). Its energy shifts toward lower binding energy for thinner films, revealing better substrate screening.¹⁰ In the 2-ML film the second-layer peak binding energy is 284.74 eV. The bottom curve is from 1 ML, prepared by annealing multilayers off. Its peak is very asymmetric, with 284.15-eV binding energy and a 0.73-eV FWHM. The binding-energy shift 0.6 eV and asymmetric line shape of 1 ML are similar to a previous study on Cu(110).¹³ A fitting to the Doniac-Sunjic line shape convoluted with a Gaussian produces poor results. The high-binding-energy side of the main peak shows many satellite peaks for the 4-ML film. These satellite peaks are almost completely attenuated for the ML film.

It may be suspected that annealing causes a structural change such as intermixing or breaking C_{60} bonds to form chains on the Cu surface. There is no evidence of intermixing C_{60} with Cu in the bulk sample.³⁸ Moreover, bulk C_{60} becomes polymerized only under high pressure³⁹ or under high laser power density illumination.⁴⁰ The C_{60} molecules start decomposing above 500 °C on Cu(111).⁴¹ Our carbon

core-level photoemission spectrum shows no change for a submonolayer film annealed to 300 °C, thus pointing to only an ordering effect.

The origin of the C 1s asymmetric line shape associated with 1 ML may have a number of reasons. These include site variations and the creation of electron hole pairs or metallic screening.¹⁰ Since only threefold hollow sites are occupied,²⁷ the multiadsorption site broadening of the line shape can be neglected. In addition, the line shape could also be influenced by the effect of different image potential screenings of a core hole on different carbon sites of a single molecule, $1/4z$ where z is the distance from the core site to the image plane. The image plane lies near the jellium edge for a clean surface.⁴² If the image plane does not change from the clean surface position during C₆₀ monolayer adsorption, it would sit in between the whole molecule and the Cu substrate. The point-charge–metal-surface image potential is reduced by the screening of other carbon atoms and nearby molecules, and is approximated by a dielectric constant of 3.92.⁴³ The screening occurs when a core hole is created, thus it is a final-state effect. Core holes closer to the interface are better screened; therefore the ejected photoelectrons have higher kinetic energies. The different distances of carbon sites from the image plane can have up to 0.6-eV different screening energies.⁴⁴ The resulted spectrum will have an asymmetric tail toward the lower-binding-energy side, exactly opposite to the observation. This means that the image plane does not stay at its position as in a clean surface, and a chemical shift can be important on the core-level binding energy. More likely, we believe that the observed tail signifies the metallic screening, and that the C₆₀ overlayer is actually metallic, consistent with the result of valence-band photoemission. We note here that the increasing binding energy for thicker films can also be understood by this image potential interaction.

There are at least six features that can be identified in the satellite region, and these features are labeled as numbers successively. For a thick film or bulk the first peak (feature 1) at 1.9 eV from the main peak is identified as an excitation from HOMO- to LUMO-derived states.^{45,46} This transition is monopolelike, and dipole forbidden, and does not show up intensely in EELS. One can say this is a true shakeup feature. The peak at 3.7 eV (feature 3) is weak in EELS, and is probably not dipole allowed. The peaks at 4.9 and 6.0 eV (features 4 and 5) are dipole allowed π to π^* transitions, and are more complicated to interpret. The EELS experiment concludes that the peak around 6 eV is due to excitation of the π plasmon.⁴⁷ Two small shoulders at about 3 and 7.5 eV (features 2 and 6) are also observed. These satellites are observable for even a 2-ML film, but are almost completely washed out for a ML film. What remains is a very broad feature centered around the π -plasmon region. This again shows the strong interaction between the substrate and the first-layer C₆₀ molecules. These satellite peaks have recently been discussed experimentally and theoretically. It is stressed that the core hole lowers the symmetry, and the screening of core holes involves global or local charge transfer within the molecule.⁴⁵ The assignment of many of these satellites can still be interpreted as due to transition between MO's of the neutral states.

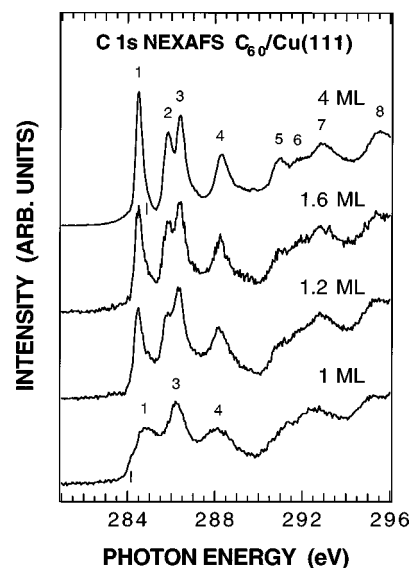


FIG. 5. Carbon 1s near-edge absorption spectra (NEXAFS) for various C₆₀ thicknesses. These spectra are normalized to the high-photon-energy sides. The ticks mark the corresponding core level binding energies for 4- and 1-ML films. For 4-ML films, peak 1 corresponds to the transition from C 1s to LUMO. The rest peaks are numbered according to the energy order. For an annealed 1-ML film, the peaks are labeled if the corresponding NEXAFS peaks for a thick film can be traced.

C. NEXAFS and a Fermi edge

The carbon NEXAFS spectra are displayed in Fig. 5, where they are normalized to the high-energy side. The peaks are labeled according to their energies. The 4-ML spectrum resembles the published results for thick films.^{48,49} The first peak at 284.5 eV is a C 1s transition to the π^* LUMO. The next three peaks at 285.8, 286.4, and 288.3 eV (peaks 2, 3, and 4) may be labeled as LUMO+1, LUMO+2, and LUMO+3, respectively, and are excitations to other π^* orbitals. Above the ionization threshold at 290 eV, the broader structures at 291.0, 291.8, 292.9, and 295.5 eV (peaks 5–8) are due to transitions to σ^* orbitals. A combined theoretical and experimental study finds that the core hole breaks the symmetry, and the absorption spectrum deviates strongly from the ground-state density of states.⁵⁰ However, the low-lying absorption peaks can still be traced back to ground-state orbitals. We shall discuss this in more detail in Sec. III E. Unlike core-level spectra, in that the peak energy shifts to lower binding energy slightly as the thickness decreases, the NEXAFS are essentially unchanged down to 2 ML (not shown). This is in part due to quite different final states of these two spectroscopies. Photoemission leaves an ionized final state with a localized core hole. The binding energy with respect to the substrate depends upon the distance to the substrate that offers image screening. On the other hand, for NEXAFS the final state is close to an excited neutral state. The excitation to the more localized final state becomes independent of the substrate screening. Further, the small mean free path of photoelectrons and Auger electrons guarantees that most of the signal comes from the outermost layer.³⁷

The 1-ML spectrum changes dramatically relative to that of a thick film. The spectrum from a 1-ML film becomes

very different. The LUMO peak becomes much more broadened and attenuated at 284.8 eV. This energy is higher than the LUMO peak energy in the thick films. The LUMO+1 peak seems to disappear or merge with LUMO+2. The LUMO+2 and LUMO+3 peaks shift down slightly to 286.2 and 288.1 eV, respectively. The 291- and 291.8-eV peaks are attenuated, and the two rest peaks shift down about 0.4 eV. This again implies the strong interaction of the C₆₀ monolayer with the Cu substrate. This downward shift in energy is consistent with K-doped C₆₀ films in that charge transfer is widely believed.⁴ If we assume the amount of charge transfer is proportional to the shift as in the case of K-doped C₆₀ films,⁴ there are approximately 1.5–2 electrons transferred to the C₆₀ molecule, consistent with results from valence-band photoemission. It is noted that the first σ^* resonance, originally at 291 eV, is more strongly attenuated than other high lying σ^* resonances. This is similar to the case of K-doped C₆₀ films.⁴ We note here that the spectra in Fig. 5 do not correspond to all of the core-level spectra shown in Fig. 4. Instead, the gradual transition between 1- and 2-ML thicknesses is emphasized.¹³ We find the spectra of 1.1 and 1.6 ML can be reproduced by a linear combination of 1- and 4-ML spectra. This shows that the electronic structure of the first layer is not much affected by the second layer on top of it, and the interaction between the first and second layers is due to a weak van der Waals force.

It has been argued that the absorption onset corresponds to the creation of a final state where a core electron has been placed in the lowest unoccupied state, i.e., at the Fermi level in a metallic system.⁵¹ In the completely screened core-level photoemission final state, a charge redistribution has taken place, where one electron has been taken from the Fermi level to screen the core hole locally. The two final states are indistinguishable, and the energy onset in absorption should correspond to the binding energy in PES.⁵² In Fig. 3, the ticks mark the binding energies of C 1s core-level photoemission of the same thickness. For the 4-ML film the core-level binding energy is above the first absorption peak (LUMO). This can be understood because the C₆₀ thick film is an insulator. The photoelectron leaving the surface creates a positive ion state, while absorption may be viewed as an excited neutral state.⁵⁰ The system is less perturbed in the latter process, thus the excitation energy is lower. It is seen in Fig. 3 that for the 1-ML film the C 1s core-level binding energy coincides with a clear step edge at the onset of the absorption spectrum. We then interpret this step edge as the transition of a carbon core electron to the unoccupied states localized within the C₆₀ overlayer right at the Fermi energy. This again suggests that the overlayer is metallic.

D. Work-function change of a ML film

It was reported in the IPES study that the work function does not change from the value of a clean Cu(111) surface for C₆₀ adsorption, and, consistently, the image state associated with the ordered overlayer appears at the same energy above the Fermi level as in the case of clean surface.¹² In the present study we check the work function by performing a photoemission measurement on the secondary edge rise and the Fermi energy cutoff. The known photon energy (He I), subtracting the total spectral width yields the absolute work

TABLE I. Work functions of clean metal surfaces and after adsorption of a monolayer of C₆₀.

Surface	Clean surface WF (eV)	WF of 1-ML C ₆₀ on surface	WF change
Cu(111) ^a	4.94	4.86	−0.08
Ni(111) ^b	5.36	4.93	−0.43
Al(110) ^c	4.35	5.25	+0.95
Al(111) ^c	4.25	5.15	+0.95
Au(110) ^d	5.37	4.82	−0.45
Rh(111) ^e	5.4 ^f	4.9	−0.5
Ta(110) ^g	4.8 ^e	5.4 ^g	+0.6 ^h

^aPresent work.

^bReference 41.

^cReference 56.

^dReference 58.

^eReference 26.

^fReference 53.

^gReference 20.

^hFor reference only, since C₆₀ decomposes on this surface at RT.

function. The obtained work function of a clean surface is 4.94 eV, the same as the tabulated value.⁵³ The work function for a C₆₀-covered Cu(111) surface is 4.86 eV, confirming that the work function changes very little. This raises a serious question. It is well known in the study of alkali adsorption on metal surfaces that charge transfer from alkali atoms to the substrate results in a large decrease of the work function.⁵⁴ Charge transfer from the substrate to the C₆₀ overlayer would increase the work function. However, the measured work function shows a slight decrease instead.

We then perform a model calculation to estimate the work-function change due to charge transfer. The work function change can be written as $\Delta\phi = 4\pi neqd = 2\pi nep$, where n is the adsorbate area density, e the electron charge, q the amount of charge transfer per adsorbed molecule, d the distance from the adsorbate to the image plane, and $p = q(2d)$ is the dipole moment per adsorbed molecule including its image charge. The polarization of a particular adsorbed molecule due to neighboring dipoles should be taken into consideration, and this tends to reduce the total dipole moment.⁵⁵ The result is a 2.9-eV work-function increase per electron transferred. For Cu(111), if 1.5 electrons transfer to the C₆₀ molecule, the work-function increase would be 4.35 eV, a huge value. So why is there almost no work-function change?

The reason is that the C₆₀ overlayer on the Cu(111) surface is metallic. It has been argued that the image plane moves from the interface to the outside of the metallic overlayer; the interface dipole layer created by charge transfer is screened out by the image plane. Therefore, the measured work function for a monolayer film is purely due to the metallic overlayer, and is not related to the interface.¹² The observed almost no work-function change is just a coincidence. We note here that the absence of a tail at the low-binding-energy side of C core-level photoemission is consistent with the induction that the image plane no longer stays at the interface. Moreover, to have an image plane at the outside of the overlayer, the overlayer itself must be metallic laterally, in consistency with the PE observation. To further

extend this idea, in Table I we compile the known work-function changes of a few systems of C_{60} chemisorption on metal substrates. It is seen that the work functions for all C_{60} -covered surface are centered around 5 eV, as pointed out before.⁵⁶ This strongly suggests that the C_{60} overlayers on these surfaces are all metallic, and that the measured work functions are the property of the metallic overlayers that give similar values regardless of the metal substrates. We then propose that charge transfer from the substrate to the overlayer plays a major role in the C_{60} -metal-surface interaction. This is likely in line with a pioneering photoemission study which stated that the energy levels of the first layer are aligned to the substrate Fermi level due to charge transfer to LUMO-derived states, despite the variety of the substrate work functions.⁷ Since the work functions are similar, the energy levels with respect to the vacuum level are also similar. We add here that for multilayers the binding energies may be more properly referenced to the vacuum level.⁵⁷

E. Comparison of NEXAFS with IPES

In addition to NEXAFS, IPES has been used to probe the unoccupied states. The latter process consists of a transition from a high-lying free-electron-like state down to a low-lying unoccupied orbital near the Fermi energy; no core state is involved. In contrast to a core-excited neutral final state in NEXAFS, the final state in IPES is a negative ion state. The presence of a core hole in NEXAFS generates an attractive potential acting on the valence-band orbitals. This effect can be discussed alternatively in terms of equivalent core or $Z+1$ approximation⁵² and pulls the ground-state levels down in energy. The resulting spectrum is also governed by the matrix element between the localized core-hole state and the perturbed unoccupied state. On the other hand, in the IPES process the final negative ion state is relatively nonlocal, and the spectrum closely resembles the density of states of the ground state, with possibly a uniform upward shift in energy levels. This has been verified for the insulating thick C_{60} films.^{46,59} A comparison of IPES with NEXAFS has been discussed in detail on molecular chemisorption systems.⁶⁰

In Table II we present a comparison of peaks in NEXAFS and IPES of thick films and a 1-ML C_{60} on Cu(111) system. The IPES data are extracted from Refs. 12 and 59 with respect to the substrate Fermi energy. The peak number is used here to avoid the confusion in assigning MO's in both techniques. For thick films the peaks in IPES have been analyzed theoretically in terms of the density of states. Peak 1 is the LUMO, or molecular orbitals of t_{1u} symmetry. Peak 2 is derived from t_{1g} . Peak 3 is a combination of molecular t_{2u} and h_g states, and a nonmolecular state with wave function localized in the cage.⁵⁹ In NEXAFS, peaks 1 and 2 are derived from t_{1u} and t_{1g} , respectively.⁵⁰ Peak 3 is mainly from t_{2u} and peak 4 has most contribution from the nonmolecular state. This is in contrast to the IPES assignment. For an annealed 1-ML film, peaks 1 and 3 are likely directly related to peaks 1 and 3 in thick-film spectrum in both NEXAFS and IPES. Peak 2 in the thick-film spectrum is most dispersive in solids,⁵⁹ and is more easily affected by chemisorption and becomes unresolved. The peak labeled 3' in IPES has no counterpart in NEXAFS. It has been identified as an image potential state associated with the ordered, metallic C_{60}

TABLE II. Comparison of peaks in NEXAFS and IPES of $C_{60}/Cu(111)$. The difference between energy levels by IPES and C 1s binding energy is displayed as (IPES-core level). The numbers in the parentheses are the energies relative to peak 1 or LUMO. The C 1s binding energies are 284.85 and 284.15 eV for a 4-ML film and a 1-ML annealed film, respectively. Most peak energies of IPES are obtained from Ref. 12. The peak 4 energy of thick-film IPES is from Ref. 59.

(a) Thick films				
peak labels	1	2	3	4
NEXAFS (eV)	284.5	285.8	286.4	288.3
	(0)	(1.3)	(1.9)	(3.8)
IPES [$E-E_F$ (eV)]	1.4	2.6	3.6	4.3
	(0)	(1.2)	(2.2)	(3.9)
IPES-core level	286.2	287.4	288.4	289.1
(b) 1 ML (annealed)				
peak labels	1	3	3'	4
NEXAFS (eV)	284.8	286.2		288.1
	(0)	(1.4)		(3.3)
IPES [$E-E_F$ (eV)]	1.5	3.0	4.1	>5
	(0)	(1.5)	(2.6)	(>3.5)
IPES-core level	285.7	287.2		

overlayer.¹² Because the image state is totally delocalized and has much weight away from the carbon atoms in the overlayer, the matrix element between the localized C 1s state and the extended image state vanishes, and cannot be detected in NEXAFS. The numbers in parentheses are energies relative to the lowest peak. It is seen that the energy differences of the two lowest peaks observed in both techniques are very similar. This justifies their correspondence. The deviation of the ground-state interpretation becomes larger for higher-lying peaks in NEXAFS. For convenience of discussion the unoccupied-state-core-level energy difference is also shown from IPES and core-level photoemission measurements. The resulting numbers can be compared directly to the absorption energies in NEXAFS for monolayer systems, but are only approximations for thick insulating films.⁶¹ It can be seen that the values of (IPES-core level) are about 1.7 and 0.9 eV larger than NEXAFS results for thick and 1-ML films respectively. This difference reflects the different screening in all three techniques. With the final state of NEXAFS being an excited neutral state, and that of core-level PES and IPES being ionic states the NEXAFS excitation energy is necessarily lower than (IPES-core level). These two energy differences can also be viewed alternatively as the unoccupied orbitals being pulled down in energy by a core hole in the NEXAFS process relative to the ground-state energies, at least for the monolayer case.⁵² The 0.8-eV reduction for the 1-ML film relative to thick films suggests that the 1-ML C_{60} overlayer has a metallic property that offers better screening on the ionic final states or on the core holes.

IV. SUMMARY

In summary, we carried out valence-band and carbon core-level PES and NEXAFS studies to probe both the oc-

cupied and unoccupied states of C_{60} adsorbed on Cu(111) surfaces. All observations point to the monolayer film being metallic, and this is due to charge transfer from the substrate to LUMO-derived states. This is consistent with previous IPES results. The amount of charge transfer can be determined independently by photoemission and NEXAFS to give 1.5–2 electrons per C_{60} molecule. We argued that the measured work function is the property of the metallic overlayer, and the dipole layer at the interface due to charge transfer is screened out by the image plane located outside the overlayer. Further, the fact that for many C_{60} -covered metal surfaces the work functions are always around 5 eV suggests all these C_{60} overlayers are metallic, and charge transfer from the substrate to the overlayer plays a major role in the C_{60} -metal-surface interaction. This is in line with the photoemission study that the energy levels of the first layer are aligned to the substrate Fermi level due to charge transfer to

LUMO-derived states despite the variety of the substrate work functions. Since the work functions are similar, the energy levels with respect to the vacuum level are also similar. Finally, we compared the data from NEXAFS and IPES, and found that core hole pulls down the unoccupied orbitals by 1.7 and 0.9 eV for thick and 1-ML films, respectively. The smaller value of the latter case reflects the better screening provided by the metallic overlayer.

ACKNOWLEDGMENTS

We acknowledge help from the staff in the SRRC, who provided technical assistance. One of us (K.D.T) is grateful to P. A. Bruhwiler for many stimulating discussions, and to P. D. Johnson and E. W. Plummer for discussions at a certain stage. This work was supported in part by the National Science Council of the ROC.

- ¹A. F. Hebard, M. J. Rosseinsky, R. C. Haddon, D. W. Murphy, S. J. Duclos, K. B. Lyons, B. Miller, J. M. Rosamilia, R. M. Fleming, A. R. Kortan, S. H. Glarum, A. V. Makhija, A. J. Muller, R. H. Eick, S. M. Zahurak, R. Tycko, G. Dabbagh, and F. A. Thiel, *Nature (London)* **350**, 600 (1991).
- ²K. Tanigaki, T. W. Ebbesen, S. Saito, J. Mizuki, J. S. Tsai, Y. Kubo, and S. Kuroshima, *Nature (London)* **352**, 222 (1991).
- ³P. J. Benning, D. M. Poirier, T. R. Ohno, Y. Chen, M. B. Jost, F. Stepniak, G. H. Kroll, J. H. Weaver, J. Fure, and R. E. Smalley, *Phys. Rev. B* **45**, 6899 (1992).
- ⁴C. T. Chen, L. H. Tjeng, P. Rudolf, G. Meigs, J. E. Rowe, J. Chen, J. P. McCauley, Jr., A. B. Smith III, A. R. McGhie, W. J. Romanow, and E. W. Plummer, *Nature (London)* **352**, 603 (1991).
- ⁵R. W. Lof, M. A. van Veenendaal, B. Koopmans, H. T. Jonkman, and G. A. Sawatzky, *Phys. Rev. Lett.* **68**, 3924 (1992).
- ⁶P. J. Benning, F. Stepniak, D. M. Poirier, J. L. Martins, J. H. Weaver, L. P. F. Chibante, and R. E. Smalley, *Phys. Rev. B* **47**, 13 843 (1993).
- ⁷T. R. Ohno, Y. Chen, S. E. Harvey, G. H. Kroll, J. H. Weaver, R. E. Haufler, and R. E. Smalley, *Phys. Rev. B* **44**, 13 747 (1991).
- ⁸S. J. Chase, W. S. Bacsa, M. G. Mitch, L. J. Philione, and J. S. Lannin, *Phys. Rev. B* **46**, 7873 (1992).
- ⁹G. K. Wertheim and D. N. E. Buchanan, *Phys. Rev. B* **50**, 11 070 (1994).
- ¹⁰A. J. Maxwell, P. A. Bruhwiler, A. Nilsson, N. Martensson, and P. Rudolf, *Phys. Rev. B* **49**, 10 717 (1994).
- ¹¹A. J. Maxwell, P. A. Bruhwiler, S. Andersson, D. Arvantis, B. Hermnas, O. Karis, D. C. Mancini, N. Martensson, S. M. Gray, M. K.-J. Johansson, and L. S. O. Johansson, *Phys. Rev. B* **52**, R5546 (1995).
- ¹²K.-D. Tsuei and P. D. Johnson, *Solid State Commun.* **101**, 337 (1997).
- ¹³J. E. Rowe, P. Rudolf, L. H. Tjeng, R. A. Malic, G. Meigs, C. T. Chen, J. Chen, and E. W. Plummer, *Int. J. Mod. Phys. B* **6**, 3909 (1992).
- ¹⁴D. W. Owens, C. M. Aldao, D. M. Poirier, and J. H. Weaver, *Phys. Rev. B* **51**, 17 068 (1995).
- ¹⁵M. R. C. Hunt, S. Modesti, P. Rudolf, and R. E. Palmer, *Phys. Rev. B* **51**, 10 039 (1995).
- ¹⁶S. Modesti, S. Cerasari, and P. Rudolf, *Phys. Rev. Lett.* **71**, 2469 (1993).
- ¹⁷C. Cepek, A. Goldoni, and S. Modesti, *Phys. Rev. B* **53**, 7466 (1996).
- ¹⁸A. V. Hamza, J. Dykes, W. D. Mosley, L. Dinh, and M. Balooch, *Surf. Sci.* **318**, 368 (1994).
- ¹⁹A. F. Hebard, C. B. Eom, Y. Iwasa, K. B. Lyons, G. A. Thomas, D. H. Rapkine, R. M. Fleming, R. C. Haddon, J. M. Phillips, J. H. Marchall, and R. H. Eick, *Phys. Rev. B* **50**, 17 740 (1994).
- ²⁰M. W. Ruckman, B. Xia, and S. L. Qiu, *Phys. Rev. B* **48**, 15 457 (1993).
- ²¹G. K. Wertheim and D. N. E. Buchanan, *Solid State Commun.* **88**, 97 (1993).
- ²²M. Pedio, M. L. Grilli, C. Ottaviani, M. Capozzi, C. Quaresima, P. Perfetti, P. A. Thiry, R. Caudano, and P. Rudolf, *J. Electron Spectrosc. Relat. Phenom.* **76**, 405 (1995).
- ²³T. R. Ohno, Y. Chen, S. E. Harvey, G. H. Kroll, P. J. Benning, J. H. Weaver, L. P. F. Chibante, and R. E. Smalley, *Phys. Rev. B* **47**, 2389 (1993).
- ²⁴J. Kovac, G. Scarel, O. Sakho, and M. Sancrotti, *J. Electron Spectrosc. Relat. Phenom.* **76**, 405 (1995).
- ²⁵S. C. Wu, K. Xun, J. Z. Deng, J. Yao, F. Q. Liu, S. H. Lu, Z. Q. Wang, R. S. Han, and Z. N. Gu, *Phys. Rev. B* **47**, 13 830 (1993).
- ²⁶A. Sellidj and B. E. Koel, *J. Phys. Chem.* **97**, 10 076 (1993); L. Q. Jiang and B. E. Koel, *Phys. Rev. Lett.* **72**, 140 (1993).
- ²⁷K. Motai, T. Hashizume, H. Shinohara, Y. Saito, H. Pickering, Y. Nishina, and T. Sakurai, *Jpn. J. Appl. Phys.* **32**, L450 (1993); T. Hashizume, K. Motai, X. D. Wang, H. Shinohara, Y. Saito, Y. Maruyama, K. Ohno, Y. Kawazoe, Y. Nishina, H. Pickering, Y. Kuk, and T. Sakurai, *Phys. Rev. Lett.* **71**, 2959 (1993).
- ²⁸J. K. Gimzewski, S. Modesti, T. David, and R. Schlittler, *J. Vac. Sci. Technol. B* **12**, 1942 (1994).
- ²⁹E. Altman and R. Colton, *Surf. Sci.* **279**, 49 (1992); E. Altman and R. Colton, *Phys. Rev. B* **48**, 18 244 (1993).
- ³⁰K. Gimzewski, S. Modesti, and R. Schlittler, *Phys. Rev. Lett.* **72**, 1036 (1994).
- ³¹Y. Kuk, D. K. Kim, Y. D. Suh, K. H. Park, H. P. Noh, S. J. Oh, and S. K. Kim, *Phys. Rev. Lett.* **70**, 1948 (1993).
- ³²Many STM studies of fullerenes on both metal and semiconductor surfaces can be found in the review article by T. Sakurai,

- X.-D. Wang, Q. K. Xue, Y. Hasegawa, T. Hashizume, and H. Shinohara, *Prog. Surf. Sci.* **51**, 263 (1996).
- ³³B.-S. Fang, T.-S. Chien, H.-H. Chen, S.-J. Jong, L.-J. Lai, and W.-S. Lo, *Nucl. Instrum. Methods Phys. Res.* **369**, 322 (1996).
- ³⁴G. M. Watson, P. A. Bruhwiler, E. W. Plummer, H.-J. Sagner, and K.-H. Frank, *Phys. Rev. Lett.* **65**, 468 (1990).
- ³⁵P. J. Benning, D. M. Poirier, N. Troullier, J. L. Martins, J. H. Weaver, R. E. Hauffler, L. P. F. Chibante, and R. E. Smalley, *Phys. Rev. B* **44**, 1962 (1991).
- ³⁶G. Gensterblum, J.-J. Pireaux, P. A. Thiry, R. Caudano, T. Buslaps, R. L. Johnson, G. Le Lay, V. Aristov, R. Gunther, A. Taleb-Ibrahimi, G. Indlekofer, and Y. Petroff, *Phys. Rev. B* **48**, 14 756 (1993).
- ³⁷G. K. Wertheim, D. N. E. Buchanan, E. E. Chaban, and J. E. Rowe, *Solid State Commun.* **83**, 785 (1992).
- ³⁸J. E. Fischer (private communication).
- ³⁹H. Yamawaki, M. Yoshida, S. Usuba, H. Yokoi, S. Fujiwara, K. Ruoff, R. Malhotra, and D. Lorents, *J. Phys. Chem.* **97**, 11 161 (1992).
- ⁴⁰P. Zhou, Z. H. Dong, A. M. Rao, and P. C. Eklund, *Chem. Phys. Lett.* **211**, 337 (1993).
- ⁴¹K.-D. Tsuei *et al.* (unpublished).
- ⁴²N. V. Smith, C. T. Chen, and M. Weinert, *Phys. Rev. B* **40**, 7565 (1989).
- ⁴³E. Shirley and S. G. Louie, *Phys. Rev. Lett.* **71**, 133 (1993); S. G. Louie and E. Shirley, *J. Phys. Chem. Solids* **54**, 1767 (1993).
- ⁴⁴In a recent calculation of core-hole screening in C₆₀ films by E. Rotenberg, C. Enkvist, P. A. Bruhwiler, A. J. Andrews, and N. Martensson, *Phys. Rev. B* **54**, R5279 (1996), it was concluded that the core hole appears from the outside to be centered on the C₆₀ cage. However, whether this may apply to our monolayer case or not does not affect our conclusion.
- ⁴⁵C. Enkvist, S. Lunell, B. Sjogren, S. Svensson, P. A. Bruhwiler, A. Nilsson, A. Maxwell, and N. Martensson, *Phys. Rev. B* **48**, 14 629 (1993).
- ⁴⁶J. H. Weaver, J. L. Martins, T. Komeda, Y. Chen, T. R. Ohno, G. H. Kroll, N. Troullier, R. H. Hauffler, and R. E. Smalley, *Phys. Rev. Lett.* **66**, 1741 (1991); P. J. Benning, D. M. Poirier, T. R. Ohno, Y. Chen, M. B. Jost, F. Stepniak, J. Fure, and R. E. Smalley, *Phys. Rev. B* **45**, 6899 (1992); S. Krummacker, M. Biermann, M. Neeb, A. Liebsch, and W. Eberhardt, *ibid.* **48**, 8424 (1993).
- ⁴⁷G. Gensterblum, J. J. Pireaux, P. A. Thiry, R. Caudano, J. P. Vigneron, Ph. Lambin, A. A. Lucas, and W. Kratschmer, *Phys. Rev. Lett.* **67**, 2171 (1991).
- ⁴⁸L. J. Terminello, D. K. Shuh, F. J. Himpsel, D. A. Lapiano-Smith, J. Stohr, D. S. Bethune, and G. Meijer, *Chem. Phys. Lett.* **182**, 491 (1991).
- ⁴⁹P. A. Bruhwiler, A. J. Maxwell, P. Rudolf, C. D. Gutleben, B. Watsberg, and N. Martensson, *Phys. Rev. Lett.* **71**, 3721 (1993).
- ⁵⁰B. Wastberg, S. Lunell, C. Enkvist, P. A. Bruhwiler, A. J. Maxwell, and N. Martensson, *Phys. Rev. B* **50**, 13 031 (1994).
- ⁵¹J. Stohr and R. Jaeger, *Phys. Rev. B* **26**, 4111 (1982).
- ⁵²A. Nilsson, O. Bjorneholm, E. O. F. Zdansky, H. Tillborg, N. Martensson, J. N. Andersen, and R. Nyholm, *Chem. Phys. Lett.* **197**, 12 (1992).
- ⁵³*CRC Handbook of Chemistry and Physics*, 75th ed. (CRC, Boca Raton, FL, 1995).
- ⁵⁴For example, see *Physics and Chemistry of Alkali Metal Adsorption*, edited by H. P. Bonzel, A. M. Bradshaw, and G. Ertl (Elsevier, Amsterdam, 1989).
- ⁵⁵B. N. J. Persson and L. H. Dubois, *Phys. Rev. B* **39**, 8220 (1989). Here we assume the transferred charge spherically distributes on the molecule as in Ref. 7; the image plane lies in between the C₆₀ overlayer and the substrate, and the distance from the adsorbate to the image plane is 4 Å. A dielectric constant of 3.92 is used as in Ref. 43, from which the molecular polarizability is obtained using Clausius-Mossotti equation. [W. D. Jackson, *Classical Electrodynamics*, 2nd ed. (Wiley, New York, 1978), p. 155.]
- ⁵⁶A. J. Maxwell, Ph.D. dissertation, Uppsala University, 1996.
- ⁵⁷A. J. Maxwell, P. A. Bruhwiler, D. Arvanitis, J. Hasselstrom, and N. Martensson, *Chem. Phys. Lett.* **260**, 71 (1996).
- ⁵⁸P. Rudolf, S. Cerasari, and S. Modesti (unpublished), as quoted in Ref. 57.
- ⁵⁹M. B. Jost, N. Troullier, D. M. Poirier, J. L. Martins, J. H. Weaver, L. P. F. Chibante, and R. E. Smalley, *Phys. Rev. B* **44**, 1966 (1991).
- ⁶⁰P. D. Johnson and S. L. Hulbert, *Phys. Rev. B* **35**, 9427 (1987).
- ⁶¹For a ML film we could also subtract core-level binding energy from NEXAFS peak energy, and compare the result with IPES peak energy as in Sec. III C. This would yield the same conclusion. For thick films both the C core-level binding energy and IPE peak energy increase with increasing thickness. Strictly speaking, for the insulating thick films the vacuum level is a better reference. We find no change of work function between a ML film and a thick film. However, this reference term cancels in the quantity of (IPES-core level).